Microbial Pathogenesis 135 (2019) 103609

Contents lists available at ScienceDirect

Microbial Pathogenesis

journal homepage: www.elsevier.com/locate/micpath

Green synthesis, characterization and antibacterial activity of silver nanoparticles by *Malus domestica* and its cytotoxic effect on (MCF-7) cell line

Mariadoss Arokia Vijaya Anand[a,**], Ramachandran Vinayagam[a], Shalini Vijayakumar[a], Agilan Balupillai[a], Franklin Jebaraj Herbert[b], Sanjay Kumar[b], Alaa Y. Ghidan[c], Tawfiq M. Al-Antary[c], Ernest David[a,*]

[a] Department of Biotechnology, Thiruvalluvar University, Vellore, 632 115, Tamil Nadu, India
[b] Centre for Stem Cell Research, Christian Medical College, Bagayam, Vellore, Tamil Nadu, 632002, India
[c] Department of Plant Protection, School of Agriculture, The University of Jordan, Amman, 11942, Jordan

ARTICLE INFO

Keywords:
Silver nanoparticles
M.domestica
Antioxidants
Multidrug-resistant
Antimicrobial activity
Cytotoxicity

ABSTRACT

This article reports the utilization of *Malus domestica* for the synthesis of silver nanoparticles (AgNPs) with cytotoxic activity against the Michigan Cancer Foundation-7 (MCF-7) cell line as well as their antibacterial and radical scavenging potential. The biosynthesized AgNPs were confirmed using various analytical characterization techniques. The cytotoxic effect of *Malus domestica*-AgNPs (*M.d*-AgNPs) was studied by MTT assay and scavenging efficacy was assessed by DPPH, nitric oxide radical and phosphomolybdate assays. Furthermore, green synthesized nanoparticles were evaluated for their antibacterial activity against multidrug resistant-clinical isolates. *M.d*-AgNPs were observed to be almost spherical in shape with an average diameter from 50 to 107.3 nm as assessed by TEM and DLS. *M.d*-AgNPs revealed the dose-dependent antioxidant activity and antimicrobial activity against multidrug-resistant bacterial strain *viz. Enterobacter aerogenes, Klebsiella pneumoniae, Pseudomonas aeruginosa,* and *Escherichia coli*. Also, *in vitro* studies revealed dose-dependent cytotoxic effects of *M.d*-AgNPs treated MCF-7 cell line. The data strongly suggest that *M.d*-AgNPs had a potential antioxidant, antimicrobial and cytotoxicity activity.

1. Introduction

The tremendous growth in nanotechnology has opened a new-fangled window in materials science, physical science, biological science, and engineering. It deals with the synthesis of nanomaterials, having at least one diameter measuring ≤ 100 nm of different physiochemical compositions [1]. Nanomaterials offer several benefits for environment and compatibility for biomedical applications such as biosensors, drug, gene delivery, diagnostic tools and cancer treatment which have extensively studied throughout the past decade, like engineering as catalyst and optics [2]. Currently, silver nanoparticles (AgNPs) gained importance, owing to its advantages and versatile potentials such as antioxidant, antimicrobial, pharmaceuticals, anti-angiogenic, wound healing, anti-inflammatory activity and anticancer activity [3]. AgNPs produced by the biological method has a considerable significance owing to the natural abundance of renewable, cost-effective, those by implementing the green chemistry principles [4]. A number of studies have been proved the antimicrobial activity of AgNPs against pathogenic and multidrug-resistant microorganisms [5]. The plant-mediated synthesis of AgNPs has become increasingly recognized as a mean to produce cytotoxic agents to fight various cancer cell lines [6]. However, the molecular mechanism involved in the cytotoxicity of AgNPs against cancer cells is still under to clarify.

Apple is the second most consumed fruit in the world. Apple is a *pomaceous* fruit species of *Malus domestica* in the Rosaceae family (Fig. 1). Apples possess abundant therapeutic benefits and apple peels are highly packed with powerful polyphenolic compounds which are beneficial to human health [7]. Studies conducted in the past few years have also demonstrated that apples are one of the main contributors of nutritional phytochemicals in the human diet and are proved to be a natural source of phenolic compounds [8]. Recent studies have shown that apple consumption to correlate with a decreased risk of developing type 2 diabetes and cardiovascular disease [9]. Also, it has been revealed that the wax apple inhibiting oxidative stress and a pro-inflammatory cytokine, and activating anti-apoptotic proteins in diabetic rats [10]. Eberhardt et al. (2000) reported that apple peel has been

* Corresponding author. Department of Biotechnology, Thiruvalluvar University, Serkadu, Vellore, 632115, Tamil Nadu, India.
** Corresponding author. Department of Biotechnology, Thiruvalluvar University, Serkadu, Vellore, 632115, Tamil Nadu, India.
E-mail addresses: mavijaibt@gmail.com (A.V.A. Mariadoss), ernestdavid2009@gmail.com (D. Ernest).

https://doi.org/10.1016/j.micpath.2019.103609
Received 24 October 2018; Received in revised form 20 June 2019; Accepted 21 June 2019
Available online 24 June 2019
0882-4010/

Fig. 1. ***Malus domestica***.

found to have a potent antioxidant activity, anti-proliferative effects in breast cancer cells and it can greatly inhibit the growth of liver cancer and colon cancer cells [11]. In addition, apple components have chemopreventive properties in breast cancer. In this research, apple polysaccharides have been possessed to affect breast cancer cell growth or to induce apoptosis [12]. However, in the past *M.domestica* is not synthesized to any other biologically active components. Hence, the present study was undertaken for the first time on the synthesis of AgNPs from *M.domestica* extract for antioxidant, antibacterial and cytotoxic activities.

2. Materials and methods

2.1. Chemicals

Silver nitrate ($AgNO_3$), nutrient agar, Mueller Hinton agar, brain-heart-infusion broth, 10% fetal bovine serum (FBS), dimethyl sulfoxide (DMSO), ascorbic acid, methyl thiazolyl diphenyl-tetrazolium bromide (MTT), ciprofloxacin, chloramphenicol, phosphate buffer saline (PBS), sucrose, and deionized water used in this investigation were acquired from Himedia laboratories (Bangalore, India) and S.D fine chemicals Ltd (Mumbai, India). All other reagents were of analytical grade and obtained from commercial sources.

2.2. Plant materials

Approximately 360 g (fresh weight) of *M.domestica* were purchased from a local market in Vellore, Tamilnadu, India. *M.domestica* extract was prepared by cutting it into small pieces, which were then thoroughly washed with running tap water, and milled into powders by employing that were stored at −20 °C. The freeze-dried powder was also used for phytochemical screening and *in vitro* antioxidant assay as described below.

2.3. Phytochemical screening and in vitro antioxidant activity of M.domestica extract

The qualitative phytochemical screening (alkaloid, saponins, phlobatannins, glycosides, flavonoids, steroids, sterols and triterpenoids) was performed according to previous reports [13]. *In vitro* antioxidant activity, including DPPH, Phosphomolybdate, and nitric oxide radical inhibition activity also explored according to earlier reports [14]. After the preliminary phytochemical screening and antioxidant activity of *M.domestica* was further use in the synthesis of AgNPs.

2.4. Preparation of AgNPs from M.domestica extract

About 100 g of the freeze-dried apple pulp was placed in 200 mL of deionized water, which was heated for 1 h at 80 °C. The extract was filtered using filter paper, and the filtrate was later used as the reducing agent for AgNPs preparation. The synthesis of *M.d*-AgNPs was carried out by using 20 mL of the *M.domestica* extract in 180 mL of 0.1 M aqueous $AgNO_3$ solution. The mixture was stirred and heated at up to 80 °C for different durations and the colour changes were observed. The achieved NPs were well dispersed in deionized water by sonication and used for characterization studies and experiments.

2.5. Characterization of M.d-AgNPs

Physicochemical features of biosynthesized NPs were analyzed by performing UV–Vis spectroscopy (Elico SL 196, Hyderabad, India). The crystalline nature of the *M.d*-AgNPs was analyzed by X-ray diffractometer (X'pert-pro PANalytical, Netherland) operated at 40 keV with Cu κα radiation in θ-2θ. The particle size was measured using particle size analyzer (Horiba-DLS-7100E, Japan). The functional organic molecules from the *M.d*-AgNPs were determined using Fourier-transform infrared spectroscopy (FTIR PerkinElmer, USA). The morphological features of *M.d*-AgNPs were characterized by scanning electron microscope (Hitachi, Japan), Transmission electron microscope (JEOL-JSM 1200EX, Japan).

2.6. Antimicrobial susceptibility test

The antibacterial efficacy of green synthesized *M.d*-AgNPs was tested against multi-drug resistant-clinical isolates such as *Klebsiella pneumoniae, Escherichia coli, Pseudomonas aeruginosa,* and *Enterobacter aerogenes* were obtained from Sri Narayani Hospital & Research Centre, Vellore, Tamil Nadu, India (Table 1). Stock cultures were maintained at 4 °C on agar slants of nutrient media. Prior to the experiment, the isolated bacterial strains were spread on Mueller-Hinton agar plates. Wells were made in a diameter of 6 mm using a sterile cork borer and loaded with different concentration of *M.d*-AgNPs (50 µg, 100 µg, 250 µg, and 500 µg/mL) over the agar plate. 20 µg of ciprofloxacin/chloramphenicol was used as a positive control. The test plates were incubated for 24 h at 37 °C. The zone of inhibition (mm in diameter) was read and taken as the action against the MDR strains.

Table 1
Multi drug resistance pattern clinical isolates.

MDR	Source	Drug resistance	Drug sensitive
Escherichia coli	Urine	Ampicillin, Amikacin, Amoxyclav, Aztreonam, Cefepime, Ceftazidime, Cefoxitin, Ciprofloxacin,Gentamicin, Meropenem, Piperacillin and Tazobactam	Chloramphenicol
Klebsiella pneumoniae	Pleural Fluid	Ampicillin, Amikacin, Amoxyclav, Aztreonam, Ceftazidime, Cefepmie, Cefoxitin, Ciprofloxacin, Gentamicin, Mipenem, Meropenem and Piperacillin	Chloramphenicol
Pseudomonas aeruginosa	Pus	Amikacin, Cefepime, Cefotaxime Gentamicin, Meropenem, Netilmicin and Tetracycline	Ciprofloxacin
Enterobacter aerogenes	Urine	Amikacin, Ceftazidime, Cefepime, Ciprofloxacin, Ertapenem, Gentamicin, Imipenem, Meropenem Norfloxacin, Ofloxacin, Tigecycline and Tetracycline	Chloramphenicol

2.7. Bacterial inhibition assay

The minimum inhibitory concentration (MIC) of green synthesized AgNPs from *M.domestica* was screened by microtiter plate assay. Briefly, *M.d*-AgNPs were dissolved in 10% DMSO. The initial test concentration was serially diluted in a 96 well plate and inoculated with 5 µL of a suspension containing $10 \times ^{8}$ CFU mL of bacterial load (*K.pneumoniae, E.coli, P.aeruginosa,* and *E.aerogenes*). Then the plates were incubated for 24 h at 37 °C for bacterial growth. The turbidity intensity of each well was read at 600 nm and compared with the untreated control. The MIC of *M.d*-AgNPs was determined as the lowest concentration of the *M.d*-AgNPs inhibiting the visual growth of the clinical MDR strains.

2.8. Biofilm formation assay

Biofilm formation assay was performed in flat-bottomed 6-well plates on the basis of MIC results. Clinical MDR strains of *E.aerogenes* and *K.pneumoniae* was selected for this assay. Briefly, an overnight culture of bacterial strains of *E.aerogenes* and *K.pneumoniae* (0.6 OD at 600 nm) was grown in Brain-Heart infusion broth supplemented with 1% (wt/vol) sucrose and incubated at 37 °C for 24 h along with the IC_{50} concentration of *M.d*-AgNPs. After incubation, detached cells, and media components from each well were discharged by thrice washing of sterile PBS. The wells were preset with methanol for 15 min and subsequently stained with 0.1% (wt/vol) crystal violet for 5 min. Consequently, the wells were rinsed with deionized water until the blank wells appeared colorless; then 1000 µL of 95% methanol was added to each of the wells including the blank and control wells. Plates were shaken for 30 min at 37 °C and the biofilm inhibition was quantified by measuring optical density at 595 nm.

2.9. In vitrocytotoxicity assay of AgNPs

Michigan Cancer Foundation-7 (MCF-7) breast cancer cells and Human embryonic kidney cell line of HEK-293 (Non-cancerous) were procured from National Centre for Cell Science (NCCS, Pune). Exponentially growing MCF-7 and HEK-293 cells were seeded into 96-well culture plates at a density of 1×10^{4}, after the 24 h incubation, the medium was replaced with fresh medium, containing different concentrations (10, 20, 30, 40, 50, 60, 70, 80, 90 and 100 µg/mL) of *M.d*-AgNPs were then added to the cell cultures to obtain the final concentration of AgNPs and incubated for 24 h at 37 °C. Doxorubicin was used as the positive control (0.1 g/mL). After the incubation, the cells were washed with phosphate buffer solution and 100 µL of MTT (5 mg/mL in PBS) solution was added and again incubated for 4 h then the supernatant was removed and formazan crystals were dissolved in 100 µL of DMSO. Optical density was measured at 570 nm with a backdrop subtraction at 690 nm.

Table 2
Preliminary phytochemical screening of *M.domestica* extracts.

Phytochemicals	Observation	Results (+:Presence; -: absence)
Alkaloid	Reddish brown colour appeared	+
Saponins	Formation of bubbles.	+
Phlobatannins	No deposition of a red colour precipitate	–
Terpenoids	No greyish colour formed	–
Triterpenoids	Deep red colour appeared	+
Flavonoids	Formation of yellow colour precipitate	+
Glycosides	No greenish blue colour formed.	–
Steroids	Red colour formed	+
Sterols	Bluish green colour formed.	+

2.10. Statistical analysis

The analysis was done using SPSS version 20.0 (SPSS Inc., Chicago, USA). Data were initially evaluated for homogeneity of variance and normality. Means were separated by Fisher's Least Significant Difference (LSD) test with the level of significance $p \leq 0.05$.

3. Results and discussion

3.1. Phytochemical screening of M.domestica

The preliminary phytochemicals (alkaloid, saponins, phlobatannins, glycosides, steroids, sterols and triterpenoids) screenings of aqueous *M.domestica* extract were examined and the results are shown in Table 2. *M.domestica* extract shows a high content of flavonoids, terpenoids, alkaloids, saponins, tannins, and phenolic compounds. These secondary metabolites are reported to have many biological and therapeutic potential including antioxidant, antimicrobial and anticancer activities.

3.2. Antioxidants potential of M.domestica

In vitro antioxidants potential of *M.domestica* extract was screened by DPPH, Phosphomolybdate, and nitric oxide radical inhibition assay (Table 3). *M.domestica* extract displays the highest percentage of DPPH scavenging activity at a concentration of 100 µg/mL. These results were similar to those of a previous study where nanoparticle incorporated *M.domestica* extract shows a better free radical activity [15]. Phosphomolybdate assay was proved that the *M.domestica* extract had a higher potential to scavenging activity, and its scavenging activity was compared with the standard ascorbic acid. Maximum inhibition of 73.64% was obtained at 100 µg/mL concentration of *M.domestica* extract revealing a higher antioxidant activity. For a lower concentration

Table 3
Percentage of inhibition of DPPH radical, phosphomolybdate assay and nitric oxide radical scavenging activity.

Concentrations	25 (µg/ml)	50 (µg/ml)	75 (µg/ml)	100 (µg/ml)
DPPH scavenging activity				
M.domestica extracts (%)	43.54	53.22	66.12	77.41
Ascorbic Acid (%)	48.48	57.57	69.69	81.81
Phosphomolybdate assay				
M.domestica extracts (%)	45.28	58.49	66.03	73.58
Ascorbic Acid (%)	48.57	62.85	68.57	77.14
Nitric oxide radical scavenging activity				
M.domestica extracts (%)	32.07	39.62	49.05	58.49
Ascorbic Acid (%)	37.14	48.57	57.14	71.42

DPPH radical, phosphomolybdate assay and nitric oxide radical scavenging activity of *M.domestica* extracts was calculated and compared with standard ascorbic acid. The activity increased in time and concentration dependent manner.

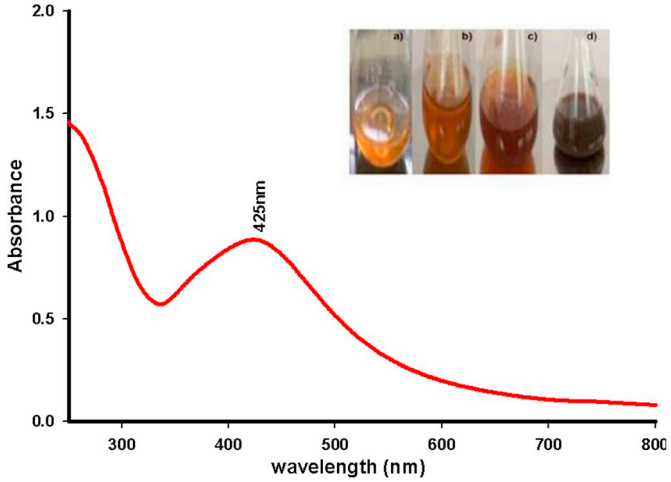

Fig. 2. UV spectrum and visible colour changes in green synthesis of AgNPs using *M.domestica* extracts. The visual observation of colour changes at different time interval (a) 0 min, (b) 5 min, (c) 10 min, and (d) 20 min.

of 25 μg/mL, 45.34% inhibition was achieved. Similarly, nitric oxide (˙NO) radical inhibition assay proved that the *M.domestica* extract has a potent scavenger of NO, and its scavenging activity was compared with the standard ascorbic acid. Maximum inhibition of 58.50% was obtained at 100 μg/mL concentration of *M.domestica* extract revealing a higher antioxidant activity. The results of this antioxidant assay revealed that *M.domestica* extract has a dose-dependent radical scavenging activity. The nitric oxide radical scavenging activity of the *M.domestica extract* showing the percentage of inhibition means that they are more potent scavengers of nitric oxide (˙NO) radical. This might be due to the antioxidant potential of *M.domestica* which competed with oxygen to react with nitric oxide thereby inhibiting the excessive

Table 4
Antimicrobial activity of *M.d*-AgNPs against human pathogenic bacteria.

Strains	Zone of inhibition in mm				
	Positive control	*M.d*-AgNPs			
	20 μg	50 μg	100 μg	250 μg	500 μg
P. aerogenosa	35 mm	10 mm	12 mm	16 mm	22 mm
E. coli	41 mm	–	–	11 mm	14 mm
E.aerogenes	29 mm	11 mm	18 mm	20 mm	24 mm
K.pneumoniae	22 mm	14 mm	17 mm	20 mm	23 mm

generation of nitrite [16]. On the basis of the considerations obtained in the present study, it is concluded that the phytochemical constituents of *M.domestica* particularly phenolic compounds exhibit high antioxidant and free radical scavenging activities. These *in vitro* assays indicate that *M.domestica* has a significant source of antioxidants, which might be useful in preventing the progress or various oxidative stresses.

3.3. Physicochemical study of green synthesized nanoparticles

3.3.1. UV–vis spectral analysis

On addition of *M.domestica* extract to the silver nitrate, as resultant the gradual change in colour towards brown which designates the formation of *M.d*-AgNPs (Fig. 1inserted). The changes in the colour from colorless to dark brown were observed within 20 min, for 80 °C which indicated the synthesis of *M.d*-AgNPs. The absorption peak was observed at 425 nm (Fig. 2) which indicated the formation of AgNPs and corresponds to surface plasmon of silver [17]. Control (*M.domestica* extract) exhibited no change in colour and the same experimental condition of incubation and there was no precipitation or aggregation was observed even after the incubation of *M.d*-AgNPs for two to three months. It shows the biosynthesized *M.d*-AgNPs was stable for three months without shifting the surface plasmon absorbance band.

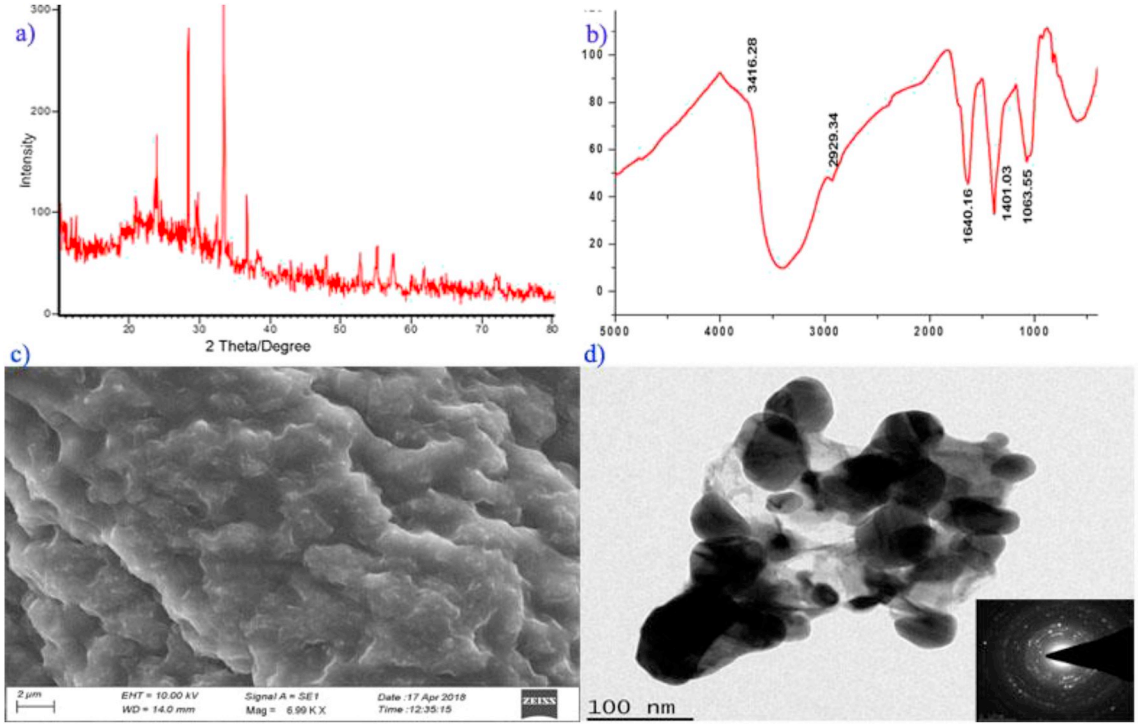

Fig. 3. (a) XRD diffraction pattern and (b) FTIR (c) SEM (d) TEM and SAED analysis of synthesized AgNPs from *M.domestica*. XRD pattern confirmed the formation of metallic AgNPs from *M.domestica*. FT-IR represents the secondary metabolites of functional groups are present on the surface of silver. SEM and TEM results confirmed the synthesized AgNPs was spherical shape and the size of AgNPs ranged from 45 to 70 nm, (Inserted Fig. 3d). SAED spots confirmed the different crystallographic planes of FCC structure of silver.

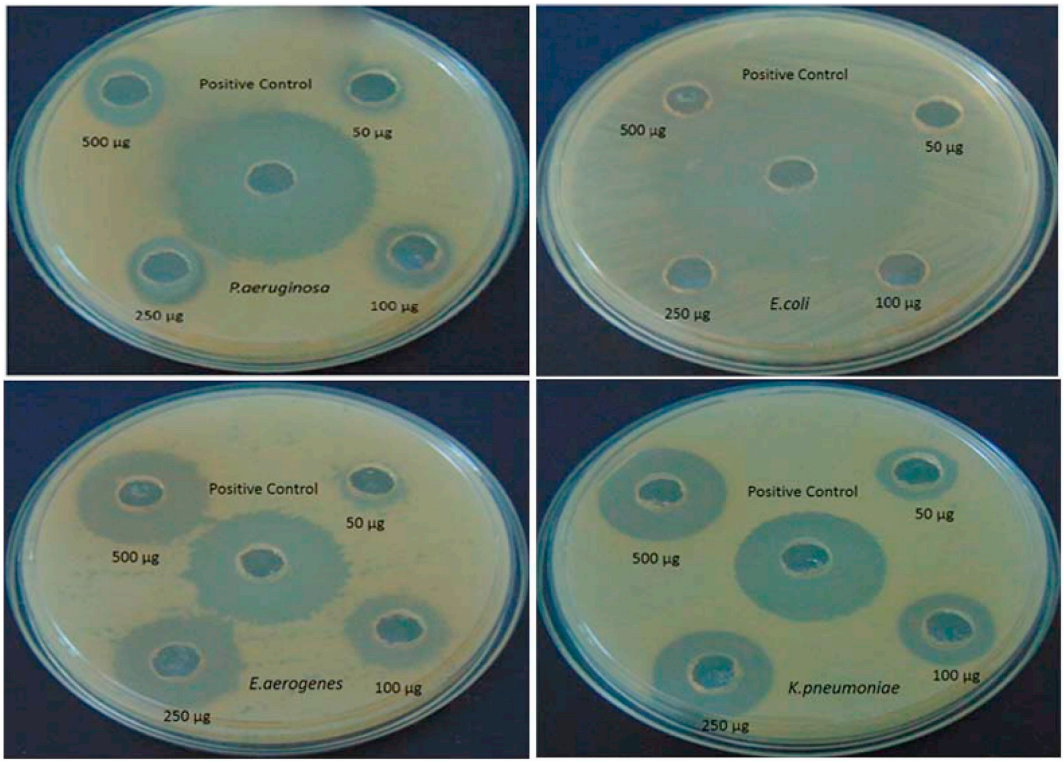

Fig. 4. The zone of inhibitory action of AgNPs synthesized using *M.domestica* against MDR clinical isolates. The zone of inhibition (mm) of different concentration of *Md*-AgNPs by disc diffusion method. The zone of inhibition was found in *E.aerogenes* (24 mm), *K.pneumoniae* (23 mm), *P.aerogenosa* (22 mm) and *E. coli* (8 mm).

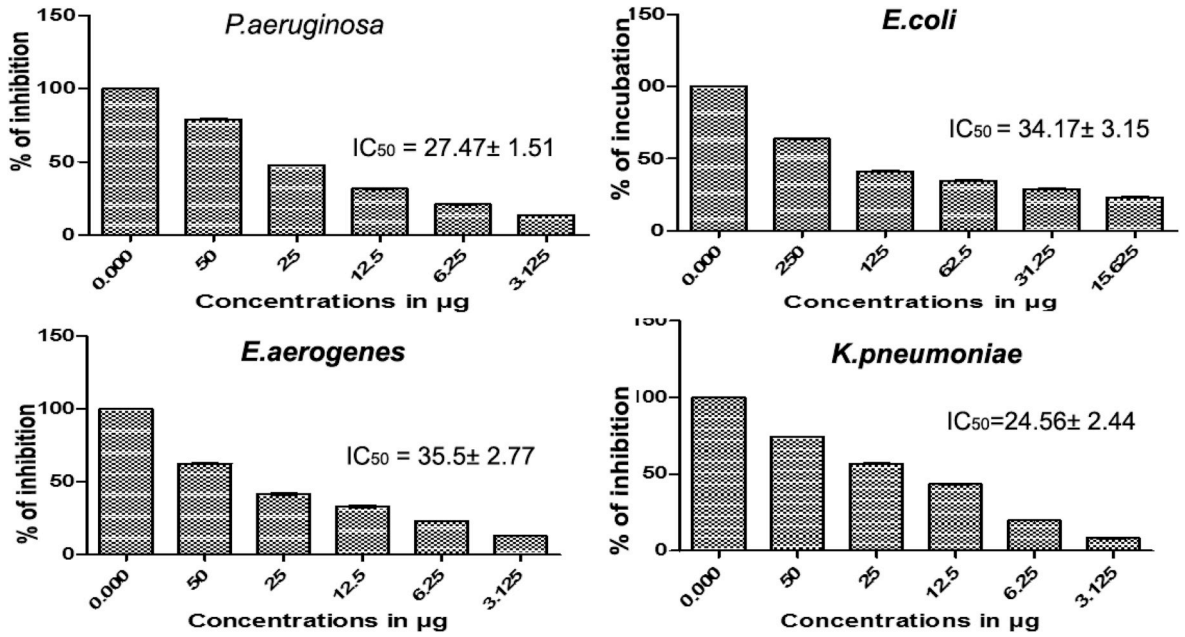

Fig. 5. The Minimum Inhibitory Concentration of *Md*-AgNPs against MDR clinical isolates. MIC of *M.d*-AgNPs was found to most inhibitory activity against clinical-isolated MDR pathogen (35.59 µg for *E.aerogenes*, 34.17 µg for *E. coli*, 27.47 µg for *P.aerogenosa,* and 24.56 µg for *K.pneumoniae*.

3.3.2. XRD and FTIR pattern of M.d-AgNPs

The crystalline nature of the fabricated *M.d*-AgNPs was investigated by XRD analysis and the result was shown in Fig. 3a. The peaks were assigned to diffraction signals of (111), (200), (220), and (311) sets of lattice plane for face-centered cubic (FCC) structure of silver. The lattice constant calculated from this pattern was 4.0869A° a value in good agreement with literature report (4.0855 A°) JSPCDS file no: 89–3722 [18], which clearly indicates that the crystalline nature of AgNPs synthesized from *M.domestica* extract. The results of FT-IR measurement of this study exhibits six different stretching bonds are shown at 3416.28 cm^{-1}, 2929.34 cm^{-1}, 1640.16 cm^{-1}, 1401.03 cm^{-1}, 1063.55 cm^{-1}, and 594.932 cm^{-1} (Fig. 3 b). The FT-IR spectrum revealed a peak at 3416.28 cm^{-1} which could be strong stretching vibrations of amine functional (N–H) and hydroxyl (O–H) group. An absorption band observed at 2929.34 cm^{-1} indicates aromatic skeletal vibrations of alkyl functional (C–H) group. An absorption band

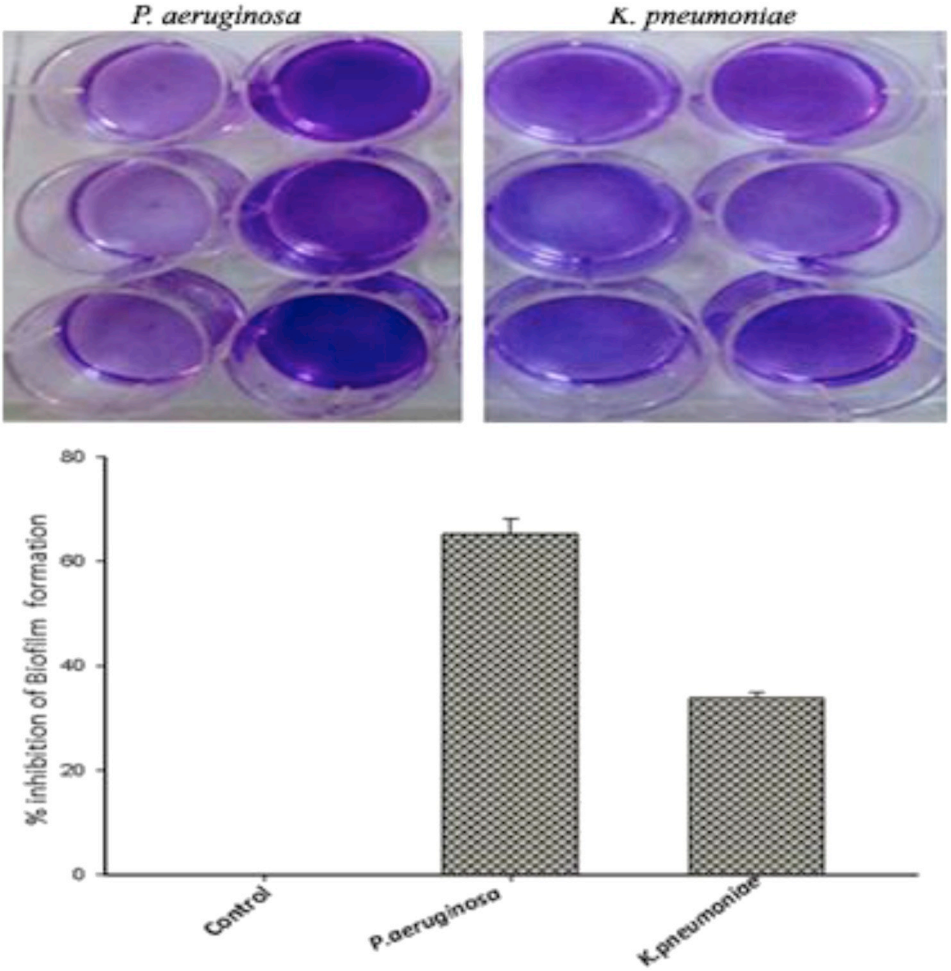

Fig. 6. Inhibition of *Md*-AgNPs against *P.aerogenosa* and *K.pneumoniae* biofilm formation. *M.d*-AgNPs reduced the biofilm formation up to 72% in *P.aerogenosa* and 33.81% in *K.pneumoniae*.

observed at 1640.16 cm^{-1} may be related to C═O symmetrical stretching or amide or amide bending, while the absorption band observed at 1401.03 cm^{-1} may represent stretching vibration (C–C). Peaks at 1063.55 cm^{-1} carbonyl group (C–O) stretching, while an absorption band observed at 594.932 cm^{-1}, indicates C–C- stretching alkane groups in amide linkages of proteins. Further, it was observed the presence of secondary metabolites such as alkaloid, saponins, triterpenoids steroids, sterols, and flavonoids act as a reducing agent, which reduces Ag^{+} to Ag^{0} and the amino group as a stabilizing agent in the green synthesis of AgNPs from aqueous *M.domestica* extract [19].

3.3.3. DLS and zeta potential analysis of M.d-AgNPs

The results of the particle size distribution curve suggest that the synthesized *M.d*-AgNPs were polydispersed in nature, with average diameter ~107 nm and the corresponding average zeta potential value is −12.9 mV (Supplementary Fig. 1). The negative potential value supports the long-term stability, good colloidal nature and high dispersity of AgNPs due to negative-negative repulsion [20].

3.3.4. Morphological analysis of M.d-AgNPs

SEM, TEM, SAED, and EDX analysis was used to study morphology, the texture of the nanoparticles and chemical composition. Morphology of synthesized *M.d*-AgNPs was examined by SEM; it was shown in Fig. 3c. TEM image was shown in Fig. 3d; it has showed particles with polydispersity and in nano size ranged from 40 to 100 nm. Fig. 3d inserted figure shows the SAED pattern of the *M.d*-AgNPs. SAED spots that linked to the different crystallographic planes of FCC structure of silver. EDX spectrum exposes strong signal in the silver region and it authorized the formation of AgNPs (Supplementary Fig. 2). Metallic silver nanocrystals commonly show typical optical absorption peak approximately at 3 KeV due to surface plasmon resonance. Based on the results ascribed from the SEM, TEM XRD, and SAED pattern suggests the polycrystalline nature of AgNPs from *M.domestica* extract.

3.4. Antibacterial activity of M.d-AgNPs

The academic community has extensively proven that AgNPs could be the best alternative to antibiotics to control the infections triggered by MDR bacterial strains [21]. In the current study, agar diffusion assay was employed to elucidate the antibacterial activity of *M.d*-AgNPs against drug-resistant clinical isolates and results were depicted in Table 4 and Fig. 4. After 24 h of incubation, a clear zone of inhibition was observed in *M.d*-AgNPs and ciprofloxacin/chloramphenicol (Positive control) loaded wells. It was found that *M.d*-AgNPs had the highest activity against *E.aerogenes* (24 mm at 500 μg/mL), *K.pneumoniae* (23 mm at 500 μg/mL), *P.aerogenosa* (22 mm at 500 μg/mL) and *E. coli* (8 mm at 500 μg/mL). The results show that MIC of *M.d*-AgNPs was found to be 35.59 μg/mL for *E.aerogenes*, 34.17 μg/mL for *E. coli*, 27.47 μg/mL for *P.aerogenosa,* and 24.56 μg for *K.pneumoniae* (Fig. 5). The findings clearly indicates that the stabilized AgNPs has excellent antimicrobial activity against MDR strain of *E.aerogenes* and the result further indicates that the antibacterial activity of the *M.d*-AgNPs is equal to the antibacterial activity of the 20 μg of positive control antibiotics. In line with the previous findings, it was confirmed that silver nanoparticles exert the same effect on MDR bacterial strains. Kasithevar

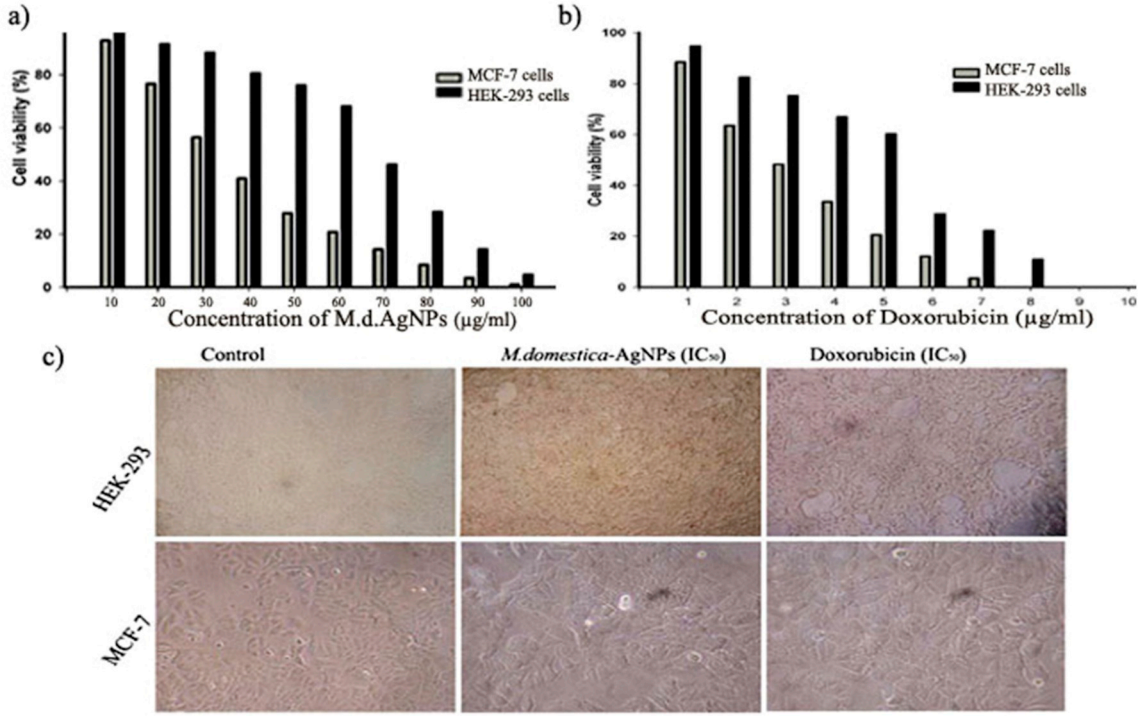

Fig. 7. Cytotoxic potential AgNPs in human breast cancer cells. The cytotoxic potential of (a) *M.d*-AgNPs and (b) doxorubicin against Non-cancerous cell lines (HEK-293) and breast cancer cell lines (MCF-7). (c) The microscopical images (20X) shows IC50 value of *M.d*-AgNPs was found to be 33.81 µg/mL MCF-7 cells and 74.95 µg/mL in HEK-293 and standard doxorubicin was found in 3.45 µg/mL in MCF-7 and 6.81 µg/mL in HEK-293 cells. Md-AgNPs significantly reduced the cancerous cell viability.

et al. (2017) studied the antibacterial activity of green synthesized AgNPs against a broad spectrum of MDR including *Pseudomonas aeruginosa, Staphylococcus aureus* and *coagulase-negative staphylococci* [22]. In this regard, it is possible to infer that AgNPs form aqueous apple extract display effective antibacterial activity as bacteriostatic and bactericidal agents against MDR bacterial growth in a dose-dependent manner.

3.5. Inhibition of biofilm formation by M.d-AgNPs

According to the report of the National Institutes of Health and Centre of Disease control, about ~65–80% infections occurred by biofilm formation microbes, amid which the drug resistance bacterium *P. aeruginosa*, *E. coli*, and the Gram-positive *Staphylococci*, *S.aureus* are the most common ones [23]. Green synthesized nanoparticles have an ability to resolve this problem. On the basis of the zone of inhibition and MIC results, it was decided to select *E.aerogenes* and *K.pneumoniae* used for biofilm assay. It was manifested that, *M.d*-AgNPs reducing the biofilm formation up to 72% in *P.aerogenosa*, whereas it reducing 33.81% in *K.pneumoniae* (Fig. 6). This result may lead to be a good alternative source of antifouling compounds. Lee et al. (2011) revealed that bioactive constituents of phloretin from apple inhibited biofilm formation *E.coli* O157:H7, and the apple fruit juice strongly inhibited the biofilm formation of *E.fecalis* and *S.mutans* [24,25]. These results go beyond previous reports, showing that silver nanoparticles from plant-derived phytochemical are capable of reducing biofilm synthesis because they can suppress the activity of the autoinducer-2 responsible for cell-to-cell communication [26]. Taken together the findings of this section suggest that the biofilm formation might have inhibited by the presence of phytochemicals in apple extract.

3.6. Cytotoxicity potential of M.d-AgNPs

In vitro cytotoxicity potential of *M.d*-AgNPs was evaluated *in* MCF-7 and HEK-293 (Fig. 7). The cytotoxicity impact on cell growth was examined at different concentration (10–100 µg/mL) and the results were expressed in inhibitory concentration (IC_{50}). The IC_{50} value of the *M.d*-AgNPs observed at the concentration of 33.81 µg/mL against MCF-7 cells and 74.95 µg/mL in HEK-293 and standard doxorubicin was found in 3.45 µg/mL in MCF-7 and 6.01 µg/mL in HEK-293 cells. The results show that there are no cytotoxic effects towards the *M.d*-AgNPs treated noncancerous cell line of HEK-293. In MCF-7 cells, The percentage of cancer cell growth inhibition was found to be high with the increasing concentrations of *M.d*-AgNPs. It shows that the cytotoxic effect of the biosynthesized AgNPs against MCF-7 was stronger than noncancerous cell line. Azizi et al. (2017) reported that the viability of cancerous and non-cancerous cells was decreased with increasing the concentration of biosynthesized AgNPs [27] the obtained result is similar to our exploration. Similarly, Moshfegh et al. (2019) has found that *Polysiphonia algae* silver nanoparticles showed apoptosis induction in MCF-7 cells [28]. Cytotoxic activity of *M.d*-AgNPs was probably due to the fact that nanoparticle might interfere with the cellular proteins and induce subsequent changes in cellular chemistry to provide a relatively high hydrophobicity inside bovine hemoglobin which causes a transition from alpha helixes to beta sheets and leads to partial unfolding and aggregation of the protein [29].

4. Conclusions

In the current study, a modest, rapid, cost-effective and eco-friendly method for green synthesis of AgNPs was effectively established using an aqueous extract of *M.domestica.* The physiochemical properties were characterized by UV–Vis spectroscopy, FTIR, DLS, XRD, SEM, TEM, and SAED techniques. The synthesized AgNPs has the ability to reduce the silver nitrate into silver which is shown by the colour change from yellow to dark brown and the zeta potential of the AgNPs −11.2 confirming the repulsion among the particles and the stability. The fabricated AgNPs were found to be very spherical shaped polydispersed nanoparticles were found in the range of 50–107 nm and the FTIR

analysis confirmed the presence of flavonoids, terpenoids, alkaloids, saponins, tannins, and phenolic compounds. It showed dose-dependent antioxidant potential and antibacterial activity against various gram-negative MDR clinical isolates. MIC values of biogenic AgNPs were observed in the range of 24.56–35.59 μg/mL against drug-resistant pathogen. Further, the findings of the cytotoxic study against human breast cancer cell lines by MTT assay exposed that *M.d*-AgNPs serve as a potential anticancer drug compared to the standard doxorubicin. These interesting consequences encourage further studies to investigate the molecular mechanism of *M.d*-AgNPs on breast cancer cells.

Conflicts of interest

The authors declare that there is no conflict of interests regarding the publication of this article.

Acknowledgments

The authors acknowledge financial support from the University Grants Commission, Government of India through the UGC-DSK Postdoctoral programme (Ref No: BL/15-16/0424). Thanks are also for the University of Jordan for the help.

Appendix A. Supplementary data

Supplementary data to this article can be found online at https://doi.org/10.1016/j.micpath.2019.103609.

References

[1] R. Emmanuel, M. Saravanan, M. Ovais, S. Padmavathy, Z.K. Shinwari, P. Prakash, Antimicrobial efficacy of drug blended biosynthesized colloidal gold nanoparticles from Justicia glauca against oral pathogens: a nanoantibiotic approach, Microb. Pathog. 113 (2017) 295–302 https://doi.org/10.1016/j.micpath.2017.10.055.

[2] A.P. Ramos, M.A.E. Cruz, C.B. Tovani, P. Ciancaglini, Biomedical applications of nanotechnology, Biophys. Rev. 9 (2017) 79–89 https://doi: 10.1007/s12551-016-0246-2.

[3] A.K. Mittal, Y. Chisti, U.C. Banerjee, Synthesis of metallic nanoparticles using plant extracts, Biotechnol. Adv. 31 (2013) 346–356 https://doi.org/10.1016/j.biotechadv.2013.01.003.

[4] M. Rai, A.P. Ingle, I. Gupta, A. Brandelli, Bioactivity of noble metal nanoparticles decorated with biopolymers and their application in drug delivery, Int. J. Pharm. 496 (2015) 159–172 https://doi.org/10.1016/j.ijpharm.2015.10.059.

[5] M. Saravanan, S.K. Barik, D. MubarakAli, P. Prakash, A. Pugazhendhi, Synthesis of silver nanoparticles from Bacillus brevis (NCIM 2533) and their antibacterial activity against pathogenic bacteria, Microb. Pathog. 116 (2018) 221–226 https://doi.org/10.1016/j.micpath.2018.01.038.

[6] I.M. Chung, I. Park, K. Seung-Hyun, M. Thiruvengadam, G. Rajakumar, Plant-mediated synthesis of silver nanoparticles: their characteristic properties and therapeutic applications, Nanoscale Res. Lett. 11 (2016) 40, https://doi.org/10.1186/s11671-016-1257-4.

[7] A.V. Anand Mariadoss, A. Krishnan Dhanabalan, H. Munusamy, K.,E. David, In Silico studies towards enhancing the anticancer activity of phytochemical phloretin against cancer drug targets, Curr. Drug Ther. 13 (2018) 174–188, https://doi.org/10.2174/1574885513666180402134054.

[8] M.A. Anand, K. Suresh, Biochemical profiling and chemopreventive activity of phloretin on 7, 12-dimethylbenz (a) anthracene induced oral carcinogenesis in male golden Syrian hamsters, Toxicol. Int. 21 (2014) 179–185 https://doi:10.4103/0971-6580.139805.

[9] X.F. Guo, B. Yang, J. Tang, J.J. Jiang, D. Li, Apple and pear consumption and type 2 diabetes mellitus risk: a meta-analysis of prospective cohort studies, Food Funct. 8 (2017) 927–934 https://doi: 10.1039/c6fo01378c.

[10] A. Khamchan, T. Paseephol, W. Hanchang, Protective effect of wax apple (Syzygium samarangense (Blume) Merr. & LM Perry) against streptozotocin-induced pancreatic β-cell damage in diabetic rats, Biomed. Pharmacother. 108 (2018) 634–645 https://doi.org/10.1016/j.biopha.2018.09.072.

[11] M.V. Eberhardt, C.Y. Lee, R.H. Liu Nutrition, Antioxidant activity of fresh apples, Nature 405 (2000) 903–914 https://doi.org/10.1038/35016151.

[12] S. D'Angelo, E. Martino, C.P. Ilisso, M.L. Bagarolo, M. Porcelli, G. Cacciapuoti, Pro-oxidant and pro-apoptotic activity of polyphenol extract from Annurca apple and its underlying mechanisms in human breast cancer cells, Int. J. Oncol. 51 (2017) 939–948 https://doi:10.3892/ijo.2017.4088.

[13] M.A. Hossain, K.A.S. AL-Raqmi, Z.H. AL-Mijizy, A.M. Weli, Q. Al-Riyami, Study of total phenol, flavonoids contents and phytochemical screening of various leaves crude extracts of locally grown Thymus vulgaris, Asian Pac. J. Trop. Biomed. 3 (2013) 705–710 https://doi.org/10.1016/S2221-1691(13)60142-2.

[14] J.K. Patra, K.H. Baek, Biosynthesis of silver nanoparticles using aqueous extract of silky hairs of corn and investigation of its antibacterial and anticandidal synergistic activity and antioxidant potential, IET Nanobiotechnol. 10 (2016) 326–333 https://doi.org/10.1049/iet-nbt.2015.0102.

[15] U. Nagaich, N. Gulati, S. Chauhan, Antioxidant and antibacterial potential of silver nanoparticles: biogenic synthesis utilizing apple extract, J. Pharm. (Lahore) 2016 (2016) 7141523, https://doi.org/10.1155/2016/7141523.

[16] H. Samsudin, R. Auras, D. Mishra, K. Dolan, G. Burgess, M. Rubino, S. Selke, H. Soto-Valdez, Migration of antioxidants from polylactic acid films: a parameter estimation approach and an overview of the current mass transfer models, Food Res. Int. 103 (2018) 515–528 https://doi.org/10.1016/j.foodres.2017.09.021.

[17] R.L. Prior, Oxygen radical absorbance capacity (ORAC): new horizons in relating dietary antioxidants/bioactives and health benefits, J. Funct. Foods 18 (2015) 797-710 https://doi.org/10.1016/j.jff.2014.12.018.

[18] R. Brause, H. Molten, K. Kleinermanns, Characterization of laser-ablated and chemically reduced silver colloids in aqueous solution by UV/VIS spectroscopy and STM/SEM microscopy, Appl. Phys. B-Lasers 75 (2002) 711–716 https://doi.org/10.1007/s00340-002-1024-3.

[19] A. Gangula, R. Podila, L. Karanam, C. Janardhana, A.M. Rao, Catalytic reduction of 4-nitrophenol using biogenic gold and silver nanoparticles derived from Breynia rhamnoides, Langmuir 27 (2011) 15268–15274, https://doi.org/10.1021/la2034559.

[20] Z. Li, J.S. Okasinski, J.D. Almer, Y. Ren, X. Zuo, Y. Sun, Quantitative determination of fragmentation kinetics and thermodynamics of colloidal silver nanowires by in situ high-energy synchrotron X-ray diffraction, Nanoscale 6 (2014) 365–370, https://doi.org/10.1039/c3nr04368a.

[21] P. Manivasagan, J. Venkatesan, K. Senthilkumar, K. Sivakumar, S.K. Kim, Biosynthesis, antimicrobial and cytotoxic effect of silver nanoparticles using a novel Nocardiopsis sp. MBRC-1, BioMed Res. Int. 2013 (2013), https://doi.org/10.1155/2013/287638.

[22] H. Nikaido, Molecular basis of bacterial outer membrane permeability revisited, Microbiol. Mol. Biol. Rev. 67 (2003) 593–656, https://doi.org/10.1128/MMBR.67.4.593-656.2003.

[23] M. Kasithevar, P. Periakaruppan, S. Muthupandian, M. Mohan, Antibacterial efficacy of silver nanoparticles against multi-drug resistant clinical isolates from post-surgical wound infections, Microb. Pathog. 107 (2017) 327–334 https://doi.org/10.1016/j.micpath.2017.04.013.

[24] M. Jamal, W. Ahmad, S. Andleeb, F. Jalil, M. Imran, M.A. Nawaz, T. Hussain, M. Ali, M. Rafiq, M.A. Kamil, Bacterial biofilm and associated infections, J. Chin. Med. Assoc. 81 (2018) 7–11 https://doi.org/10.1016/j.jcma.2017.07.012.

[25] J.H. Lee, S.C. Regmi, J.A. Kim, M.H. Cho, H. Yun, C.S. Lee, J. LeeJ, Apple flavonoid phloretin inhibits Escherichia coli O157: H7 biofilm formation and ameliorates colon inflammation in rats, Infect. Immun. 79 (2011) 4819–4827, https://doi.org/10.1128/IAI.05580-11.

[26] H.Z. Neihaya, H.H. Zaman, Investigating the effect of biosynthesized silver nanoparticles as antibiofilm on bacterial clinical isolates, Microb. Pathog. 116 (2018) 200–208 https://doi.org/10.1016/j.micpath.2018.01.024.

[27] M. Azizi, H. Ghourchian, F. Yazdian, S. Bagherifam, S. Bekhradnia, B. Nystrom B, Anti-cancerous effect of albumin coated silver nanoparticles on MDA-MB 231 human breast cancer cell line, Sci. Rep. 7 (2017) 5178, https://doi.org/10.1038/s41598-017-05461-3.

[28] A. Moshfegh, A. Jalali, A. Salehzadeh, A.S. Jozani, Biological synthesis of silver nanoparticles by cell-free extract of Polysiphonia algae and their anticancer activity against breast cancer MCF-7 cell lines, Micro & Nano Lett. (2019), https://doi.org/10.1049/mnl.2018.5260.

[29] J.V. Rogers, C.V. Parkinson, Y.W. Choi, J.L. Speshock, S.M. Hussain, A preliminary assessment of silver nanoparticle inhibition of monkeypox virus plaque formation, Nanoscale Res. Lett. 3 (2008) 129–133, https://doi.org/10.1007/s11671-008-9128-2.